REMOVAL OF FE (II) AND MN (II) FROM WASTEWATER USING NANO-CHITOSAN PREPARED FROM SHRIMP WASTE

Gamal M. Elkady[(1)], Hazem Fathallah[(1)], Moustfa Abo Elfadl[(2)], Mohamed Elsayed[(2)], Atef Selim

(1) Applied chemistry Dept., Faculty of science, Al Azhar university
(2) Water Desalination & Treatment Unit, Hydrogeochemistry Dept., Desert Research Center

ABSTRACT

The aim of present study is to find an economic way for water treatment to remove iron and manganese ions usin-g nano chitosan NCS. The chitosan prepared from shrimp waste characterized by FT-IR spectroscopy and X-Ray Diffraction XRD. It's molecular weight M.wt. and degree of acetylation DA also determined , it's removal enhanced by decreasing the size in the nano size form using ionic gelation method with sodium tripolyphosphate TPP. The morphology of the nano chitosan particles were studied using Scanning Electronic Microscopy SEM and Transmission electron microscopy TEM, pattern and investigate the adsorption properties of Nano chitosan for the removal of Fe(II) and Mn (II) ions from the aqueous phase in a batch equilibrium system. The different variables affecting the adsorption capacity such as contact time, pH of the sorption medium, and initial metal ion concentration in the feed solution were investigated on a batch adsorption basis. The maximum adsorption capacity of Fe (II) and Mn(II) was 99.8 and from 95.3%, respectively at 5 g of the adsorbent dose after 20 minutes.

Keywords (chitosan –nanoparticles- characterization -ionic gelation-ion removal- adsorption- water)

1. INTRODUCTION

Heavy metals are one of the most important categories of water pollutants, where they can be leached from their bearing rocks into groundwater Heavy metals are also produced during industrial activities and causes soil and water contamination[1]. Iron and manganese are metallic elements present in many types of rock. They are mostly present in the soluble reduced divalent form as ferrous Fe(II)and manganous Mn(II) ions. Both iron and manganese impart a strong metallic taste to the water, both cause staining and their accumulation have harmful effects on human body [2, 3]. Iron and manganese removal from water is recommended when the dissolved concentrations exceed 0.3 mg/L iron Fe(II) and 0.05 mg/L manganese Mn(II) [3]. Despite of presence of simple traditional methods for removal of heavy metals ions from wastewater Filtration, Chemical precipitation, Ion exchange, and Membrane technologies [4,5], the adsorption has been considered as one of the most efficient methods with many advantages including low cost, high efficiency, good selectivity and recyclability with various materials[6]. recently; low-cost adsorbents that are produced from wastes have been used widely[7]. Chitosan has the ability to adsorb significant amounts of metal ions over a wide range[4, 8]. Chitosan is a natural, nontoxic, biodegradable, and biocompatible polymer with antibacterial activity and has a wide range of applications in different fields such as membranes, medicine, drug delivery, hydrogels, water treatment, adhesives, food packaging, fuel cells, and surface conditioner [9].Chitosan can be prepared from shrimps and crabs waste throw several steps involves demineralization with acid solution, deprtonization with alkaline solution and deacetylation with a concentrated alkaline solution [10]. However; Chitin is made up of a linear chain of acetyl glucosamine groups while chitosan is obtained by removing enough acetyl groups (CH_3-CO) for the molecule to be soluble in most diluted acids.[11] The molecular weight(M.wt) and degree of deacetylation(DA)

can be modified during its preparation to obtain free amine as well as hydroxyl groups in chitosan structure [12]. It is known that chitosan is a weak base, insoluble in water and organic solvents, however, it is soluble in dilute aqueous acidic solution (pH < 6.5), which can convert the glucosamine units into a soluble form of protonated amine ($R–NH_3^+$)[13]. The adsorption capacity of chitosan or even natural polymer can be controlled by sorbent particle size, i.e. preparation of chitosan at nanoscale, because of unique size and large surface-to-volume ratio [14]. Among the variety of methods developed to prepare chitosan nanoparticles, ionic gelation technique has attracted considerable attention due to this process is non-toxic, organic solvent free, convenient and controllable[15]. Chitosan nanoparticles are formed in the ionic gelation due to the electrostatic interaction between the positively charged amine group of chitosan and negatively charge group of polyanion such as tripolyphosphate (TPP) [14].The advantage of the ionic gelation process is that desired size and surface charge can be modulated by right control of critical processing parameters such as chitosan to TPP weight ratio, pH, and concentration of chitosan and TPP solutions, etc. to fabricate the nanoparticle structure with optimum antimicrobial activity[16]. TPP has also been selected as a possible crosslinking agent for the preparation of chitosan nanoparticles because of its coagulation and neutralization effect.

In this work, an effective adsorbent chitosan nanoparticles were extracted from shrimp shell waste and using it in the removal of Fe(II) and Mn (II) ions from wastewater as there is a few paper used chitosan nanoparticles as an adsorbent for Fe (II) and Mn(II) removal. However; chitosan nanoparticles were prepared by ionic gelation technique in presence of TPP as crosslinker and characterized using FT-IR, XRD, SEM, and zeta sizer, the adsorption kinetics, adsorption isotherm (Langmuir and Freundlich) were studied.

2. EXPERIMENTAL AND MATERIAL

2.1. Materials

Local shrimp waste was collected and immediately washed several times with water and detergent then allowed to dry in open area under sunlight then grounded to small particles. The grounded material was transformed into chitosan via three successive steps (demineralization, deproteinization, and deacetylation).,Tripolyphosphate,acetic acid, Sodium hydroxide NaOH, Hydrochloric acid HCl, acetic acid glacial, Ferrous sulfate heptahydrate and Manganese chloride hydrate, Purchased from a local chemical company.

2.2. Methods

2.2.1. Extraction of chitosan from chitin

Firstly; demineralization and deproteinization to remove primarily calcium carbonate and disrupt the chemical bonds between chitin and proteins were generally performed by acid treatment technique using 1M HCl (1:10 w/v) and 1M NaOH (1:10 w/v) for 24 h for each at room temperature, respectively [11]. After that, the solution was filtered and the residue was washed several times with deionized water (DI) until neutral pH. However; demineralization was easily achieved because of decomposition of calcium carbonate into the water-soluble calcium salts with the release of carbon dioxide as shown in the following equation; [10, 17, 18].

$$2HCl + CaCO_3 \rightarrow CaCl_2 + H_2O + CO_2\uparrow$$

To convert chitin to chitosan, the acetyl groups were removed during the de-acetylation process, where demineralized chitin was transferred to a 60% sodium hydroxide solution. Then the solution was boiled for 2 h after that alkali solution was drained off and washed repeatedly with DI till pH was lowered to normal. Finally, chitosan was further dried at room temperature and stored for further uses [19].

2.2.2. Preparation of chitosan nanoparticles

Chitosan nanoparticles were prepared by dissolving at 0.5 g of prepared chitosan in 100 ml of 1% acetic acid (v/v), and the pH of the solution was adjusted to be 4.6 ~ 4.8 using 1N

NaOH. Chitosan nanoparticles were formed spontaneously upon addition of 3 ml chitosan solution under vigorous magnetic stirring to 1 ml of an aqueous TPP solution (0.25% w/v), with a ratio of chitosan to TPP 3:1 at room temperature. Nanoparticles were separated by centrifugation at 9000×g for 20 min [20]. Chitosan nanoparticles were extensively rinsed with DI to remove any NaOH residues and dried at 40C° for 24 h before further use or analysis [21].

3. CHARACTERIZATION

3.1.1. Characterization of chitosan

3.1.1.1. Ash value

To determine the ash value of chitosan, 1.0g of chitosan sample is placed and accurately weighed into clean, dry, pre-weighed porcelain crucible. The samples are heated in a muffle furnace preheated to 650ºC for 4 hr. The crucibles are allowed to cool in the furnace to less than 200ºC and then placed into desiccators with a vented top. Percentage of ash value is calculated using the following[22]

$$Ash\% = \frac{(W_1 - W_2)}{W_1} \times 100 \qquad (1)$$

Where, W_1 and W_2 in grams are the weight of chitosan before and after ignition, respectively

3.1.1.2. Determination of degree of deacetylation:

The degree of deacetylation (DA) was measured by the acid-base titration method with modifications. In brief, Chitosan (0.1 g) was dissolved in 30 ml HCl aqueous solution (0.1mol/l) at room temperature with 2-3 drops of methyl orange added. The red chitosan solution was titrated with 0.1mol/l NaOH solution until it turned orange. The DD was calculated by the formula

$$DD\% = \frac{C_1V_1 - C_2V_2)}{M \times 0.0994} \times 0.016 \qquad (2)$$

Where, C_1 = concentration of standard HCl aqueous solution (mol/l), C_2 = standard NaOH solution (mol/l), V_1= volume of the standard HCl aqueous solution used to dissolve chitosan (ml), V_2= volume of standard NaOH solution consumed during titration (ml), and M= weight of chitosan (g). The number 0.016 (g) is the equivalent weight of NH_2 group in 1 ml of standard 1 mol/l HCl aqueous solution and 0.0994 is the proportion of NH_2 group by weight of chitosan[23].

3.1.1.3. Determination of molecular weight

Viscosity was assessed using a Brookfield viscometer, Model DV3THBCJ0 (Brookfield Engineering Labs, made in USA). In brief, 1% chitosan solution was prepared using 1% acetic acid. The Measurement was made using a No. 5 spindle at 50 rpm at 25 C° with values reported in centipoises (cps) units[24].Intrinsic viscosity was used to calculate the viscosity average molecular weight for the prepared samples from the Mark-Houwink Sakurada equation:

$$\eta = KM^a \qquad (3)$$

where K and a are the constants for a given solute–solvent system is 0.078 and 0.76, respectively[24, 25].

3.1.1.4. FT-IR spectroscopy and XRD

FT-IR spectroscopy (Jasco FT-IR 6100,made in Japan) was used to compare and confirm the chemical conformation of standard chitosan with that of extracted chitosan. The spectra of chitosan samples were obtained with a frequency range of λ=400-4000 cm[26].The wide-angle X-ray diffraction (XRD) analysis was applied to detect the crystallinity of chitosan and nano-chitosan prepared and their patterns were recorded using PAN analytical XRD X'pert PRO).

3.2. Characterization of chitosan Nanoparticles.

The particle size distribution, The zeta potential and polydispersity index (PDI) of the chitosan nanoparticles were determined by dynamic light scattering (DLS) using a Zetasizer Nano instrument (Malvern Instruments, U.K.)Transmission electron microscopy (TEM) was used to examine size, shape, and morphologies of the nanoparticles prepared in this study. TEM micrographs of nanoparticle samples deposited on copper grids were obtained with a (JEOL-2100 Electron

Microscope), made in Japan**.**Scanning electron microscope(SEM) analysis is employed to determine the morphology of formed nanoparticle using (Quanta FEG250 SEM FEI company) SEM gives high-resolution images of the surface of a sample.

4. METAL ION UPTAKE EXPERIMENTS

4.1 Batch adsorption experiment

Batch adsorption experiments were conducted in two series of 150 ml beakers with 100 ml of iron and manganese solution at a certain concentration. The initial pH of solutions was adjusted using the required amounts of 0.1M HCl or0.1M NaOH solutions. The mixture was equilibrated with nano-chitosan at a rotation speed of 180rpm in a shaker for 120 min. All experiments were conducted at room temperature. Samples were taken at fixed time intervals to determine solution concentration. Iron and manganese concentrations in the filtrates were analyzed by ICP (ICAP 6500 Duo,thermo scientific England) A series of experiments were conducted to determine the effect of parameters such as adsorbent dose, pH, initial concentration, and contact time on equilibrium uptake of Fe (II)and Mn(II) ions by NCS. [27]Adsorption experiments for the removal of Fe (II)and Mn(II) ions were conducted in pH range of (2.5-7), adsorbent dosage (0.5-15 g/l), contact time from (0-120) min, metal concentration (10–120 mg/l) at room temperature. The adsorption kinetics and isotherms data were collected under the optimized condition of adsorbent dose, pH, and contact time. After separation by centrifugation (model) at 5000 rpm, the residual concentration of the metal ions was determined by ICP. In all of the above experiments, the adsorption values were calculated from the change in solution concentration using the following equation.[28]

$$q = (C_o - C_e) \times \frac{V}{M} \qquad (4)$$

where q is the amount (mg/g) of metal ions adsorbed by the NCS, C_o and C_e (mg/l) are the metal concentrations in the solution initially and after adsorption, respectively, V is the volume of added solution and m (g) is the mass of the adsorbent (dry) used. The removal efficiency calculated as:

$$R\% = 100 \times \frac{C_o - C_e}{C_o} \qquad (5)$$

5. RESULT AND DISCUSSION:

5.1. Characterization of chitosan and chitosan nanoparticles:

Chitosan produced from shrimp has been prepared at three molecular weights, high M.wt (51269.68 Dalton), medium M.wt (32403.67 Dalton) and low M.wt (3923 Dalton). The difference in M.wt of the obtained polymer was due to heating of the reaction temperature and time.[17] This is because the continuous heating of the polymer during the deacetylation process with NaOH causes a decrease in the molecular weight with the rising in the deacetylation degree.[25]. Based on the data produced from particle size analyzer, it was found that the lowest M.wt was chosen to be easier to resize it in the nano form, where the produced nanoparticle size was 331 nm, while the particle size of that produced from medium and high M.wt were 1562 and 3914 nm, respectively, Table 1. This is because of as the molecular weight decreased, the particle size also decreased the larger molecular size [29]. DA of chitosan and ash content of chitosan were 75 % and 4%, respectively. It is known that DA is the most parameter used for chitosan characterization, and is defined as the number of amines group in relation to the number of amides group of the polymeric chain formed as a result of removing $–CO-CH_3$ group from the chitin chain as shown in scheme (1). DA of chitosan may affect the adsorption properties for application in water and wastewater treatment, the obtained medium DA 75 % confirm that the prepared chitosan can be used as an effective adsorbent for some heavy metals [30].

Scheme (1) chitin deacetylation and chitosan structure

The structure of the prepared chitosan from chitin was confirmed by FT-IR Fig.1(b).

Where; the spectrum of the prepared chitosan shows more broad absorption bands at 3422cm^{-1} than that observed in the spectrum of chitin, therefore this broadband might be corresponded to -OH stretching vibrations of water, hydroxyls and NH_2 stretching vibrations of free amino groups. The two bands observed at 2923.56 and 2859.92 cm^{-1} corresponds to asymmetric stretching of CH_3 and CH_2 in both chitin and chitosan. The band observed at 1645.95 cm-^{1} in chitin spectrum has been split to two bands with intensity increases, which corresponds to bending vibration of NH_2 is a characteristic feature of chitosan polysaccharide and also indicates the occurrence of deacetylation. The stretching band for C-O was at 1038.48 cm^{-1}[31].

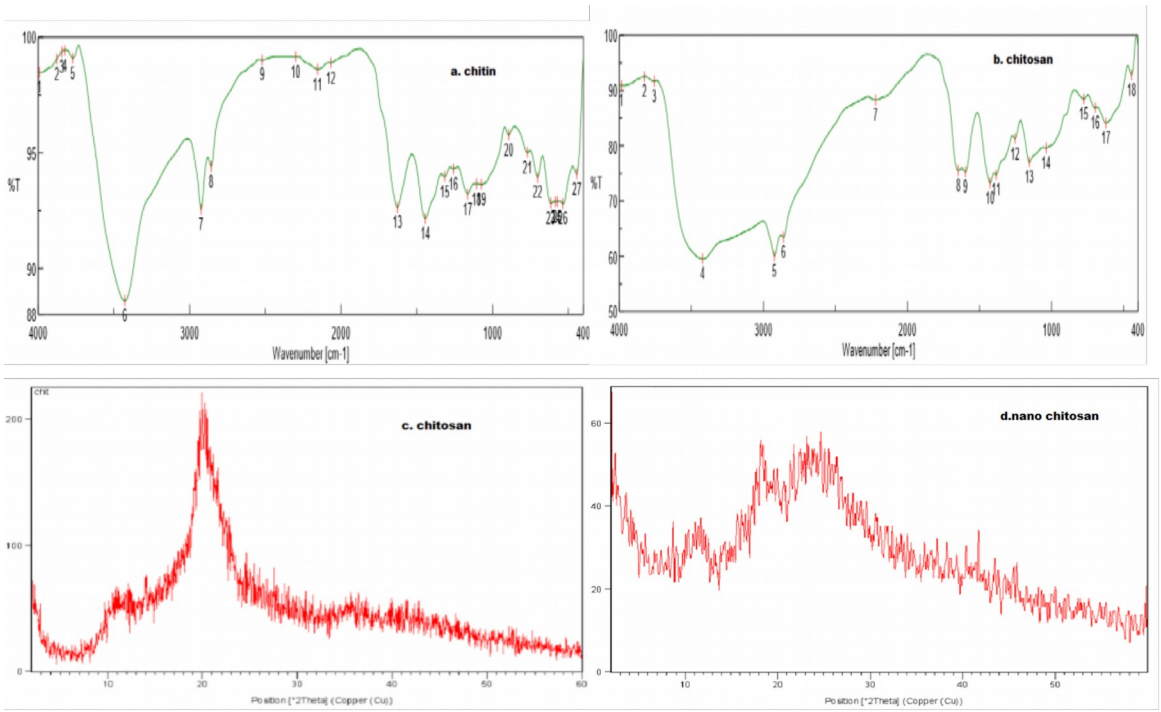

Fig.1 FT-IR spectra for (a).chitin and (b).prepared chitosan, (c) XRD for prepared chitosan and (d).nano chitosan.

Fig.1 (c,d) Shows XRD patterns of prepared chitosan and chitosan nanoparticles. Chitosan gives two characteristic peaks at 2= 10° and 20°. The crystalline structure of the chitosan nanoparticles has been fully destroyed after crosslinking with TPP, where these two peaks disappeared in the pattern of NCS, which indicates the amorphous nature, i.e. according to a previous work [32], decreasing of the polymer crystallinity results in an improvement in metal ion sorption and capacity. The decreasing of crystallinity could be due to that chitosan nanoparticles are composed of a dense network structure of interpenetrating counter ions TPP, where the polymer chains crosslink with each other by TPP. Thus the XRD pattern of chitosan nanoparticles is characteristic of an amorphous polymer[20]. The surface and stability of the prepared chitosan nanoparticles was characterized using zeta potential, it was found that the surface was shown to be positively charged (+38 mv). however, the positive zeta potential was because of the hydrogen bonds formed between the amino and hydroxyl groups of chitosan with the hydroxyl groups or oxygen atoms of water [33]. Therefore, the optimum preparation conditions was obtained by changing the ratio of chitosan to TPP as follow; (1:1), (2:1) and (3:1), respectively at pH of chitosan solution of 4.6-4.8[34]. The smallest particle size was obtained from the ratio of chitosan /TPP (3:1). These nanoparticles of chitosan were confirmed using TEM at two magnifications of 50 and 100 nm,

Fig. (2) that showed roughly spherical in shape [35]. Fig. (3) shows SEM images of chitosan nanoparticles show the morphology of the nanoparticles .Findings show that the particles size of chitosan and pdI as shown in Table1 [36]

Table 1. The particle size and Pdl for nano chitosan at different M.wt.

Type	M.wt(D)	Size (nm)	pdI
High M.wt chitosan	51269.68	3914	0.271
Mid M.wt chitosan	32403.67	1562	0.898
Low M.wt chitosan	3923	331	0.331

5.2. Factors affecting on Adsorption

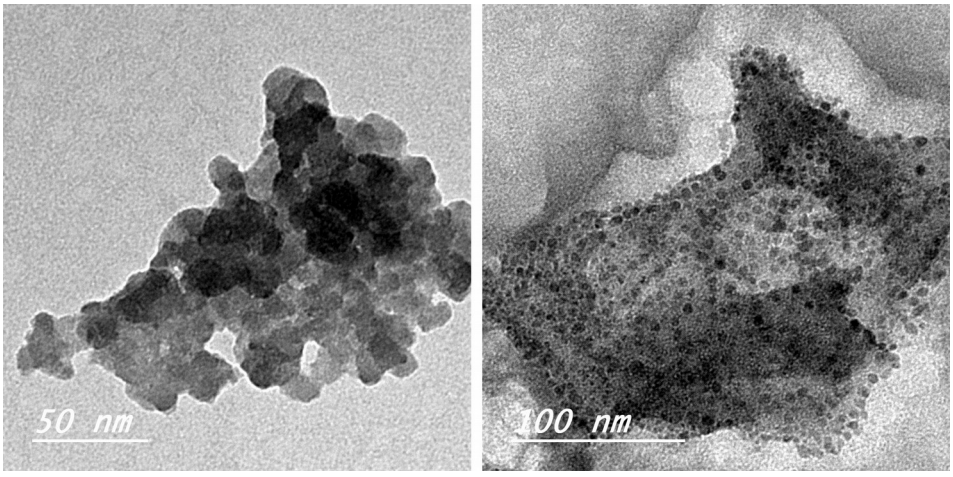

Fig.2. TEM images of chitosan nanoparticles at 50 and 100 nm.

Adsorption is separation processes in which some materials (adsorbate) are adhere from a bulk gas or liquid phase onto the surface of a porous solid (adsorbent). Batch studies use the fact that the adsorption phenomenon at the solid/liquid interface leads to a change in the concentration of the solution. Adsorption isotherms are constructed by measuring the concentration of adsorbate in the medium before and after adsorption at a fixed temperature with other different parameter such as initial concentration, adsorbent dose, contact time and pH. Several isotherm models used to describe adsorption such as Langmuir and Freundlich model can describe the distribution of metal ions on the surface of the solid phase of adsorbent. the adsorption rate is another important factor and adsorption kinetics must be taken in consider which explain how fast the chemical reaction occurs and also provide information on the factors affecting the reaction rate. two kinetic models used pseudo-first-order kinetic model and pseudo-second-order kinetic model .we used the previous factor to study the adsorption of Fe (II)and Mn(II) ions onto NCS using batch experiments [32].

Speciation of heavy metal ions and surface charge of adsorbent depends mainly upon pH of the solution. Hence, it is customary to study the effect of pH on adsorption efficiency for sorption studies [37]. However; pH must be less than that at which metal ions precipitate, i.e. pH 6 for iron and 8 for Mn, [38].The effects of pH on the removal of Fe (II) and Mn (II) were studied with the pH ranges of 2.5±0.2 to 7±0.2 with keeping other parameters constant, Fig.4 (a). From the figure, the optimum adsorption takes place at pH 4 for Fe (II) and at pH 6 for Mn(II), where the removal percent was 81.3 and 81.1, respectively. Further increase in pH leads to the precipitation of Fe (II) which inhibits the adsorption process. While, at low pH values, chitosan is positively charged with higher H^+ ion concentration, which led to protonation of amino groups that induces an electrostatic repulsion of metal cations that reduces the number of binding sites available for metallic ions [32]. In general, Fe (II) and Mn (II) ions uptake increases as the pH increases until to pH 7.

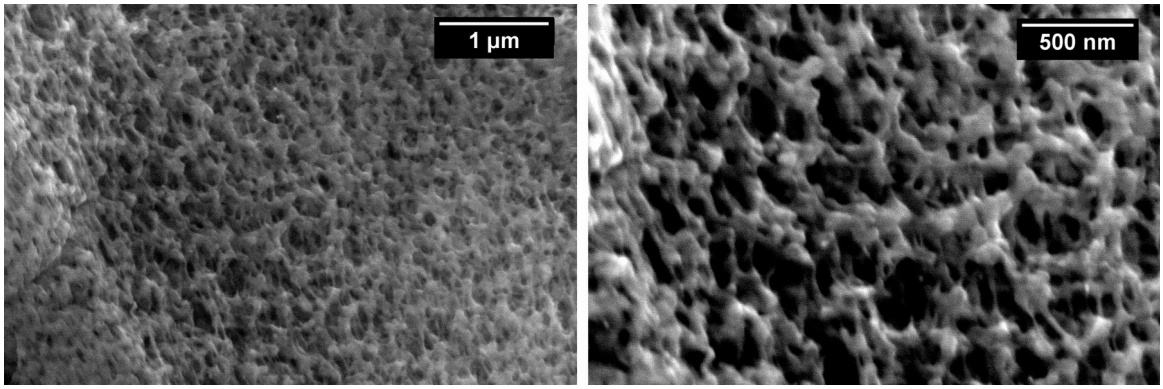

Fig.3. SEM images of chitosan nanoparticles at 1µm and 500nm.

The amount of adsorbent was one of the important parameters that strongly affect the sorption capacity. The dependence of Fe (II) and Mn(II) ions sorption on nano chitosan was studied by varying the amount of the adsorbent from 0.5 g to 15 g while keeping the other parameters such as pH4.0±0.2 for Fe (II) ions, pH 6±0.2 for Mn(II) ions metal solution volume (1000 ml), concentration (10 mg/L), and contact time (120 min) constant. Fig.4 (b) show that the removal percentage increases with increasing adsorbent dose from 92% to 99.8%.for Fe (II) and from 37.9%to 95.3% for Mn(II) ions. These increases were attributed to increasing the active sites and surface area of the chitosan nanoparticles.

Fig.4 (c) shows the effect of initial concentration of Fe (II) and Mn(II) ions onto removal efficiency, where different concentrations of the metal ions were gently shaken with 0.05 g of chitosan nanoparticles at pH of the solution 4 and 6 for Fe (II)and Mn(II) respectively. The figure shows that the removal efficiency of the metal ions decreased from 87 to 49 % and from 44.9 to 27 % for Fe (II) and Mn(II), respectively as the initial concentration increased from 20, 40, 60, 80, 100 and 120 mg/l.The removal efficiency decreased with the increase in initial metal ions concentration. The poorer uptake at higher metal concentration was resulted due to the increased ratio of the initial number of moles of metal ions to the vacant sites available in adsorbent sites which resulting in a decrease in the removal of adsorbate.

The study of contact time between adsorbent and adsorbate is necessary during adsorption process to consider the efficiency of desorption and regeneration of the adsorbent. The effect of contact time on metal ions adsorption efficiency is shown in Fig.4(d). It was observed that the adsorption rate initially increased rapidly from 5 to 20 min, and then a steady state was obtained with optimal removal efficiency within about 100 min that reached 86% and 49%for Fe (II) and Mn (II), respectively. During the process, the adsorbent surface is progressively blocked by the adsorbate molecules, becoming covered after some time. When this happens, the adsorbent cannot adsorb any more ions[39].

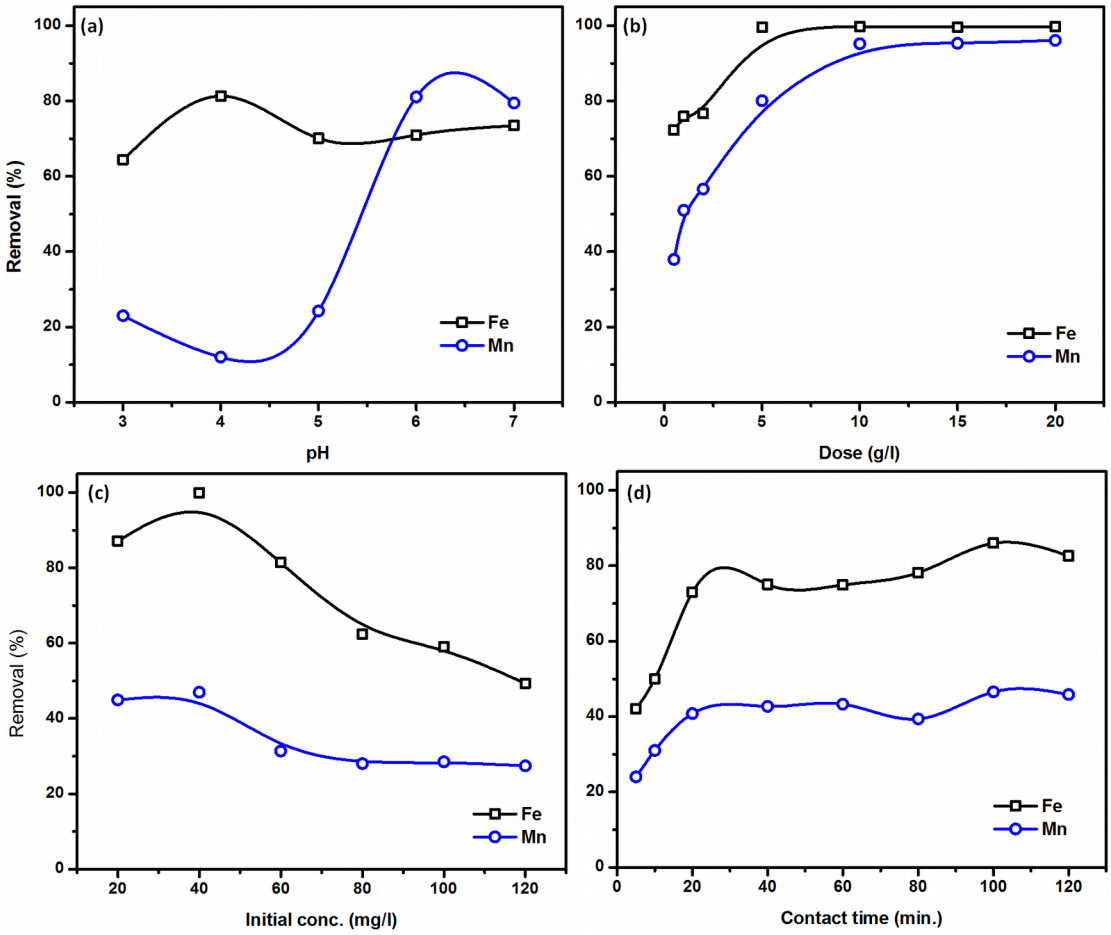

Fig.4. Effect of different adsorption parameters onto Fe (II) and Mn(II) removal efficiency using NCS adsorbent (a), pH of the aqueous solution (b), adsorbent dose (c), initial concof metal ions, and (d) contact time

5.3. Adsorption Isotherms

Adsorption isotherms are essential in order to determine the adsorption potential of the adsorbent. Figs. (4) show the experimental data of adsorption of Fe (II) and Mn (II) on NCS at different concentrations. However; Langmuir and Freundlich's equations were used to fit the experimental data. The linearized Langmuir adsorption model is shown by the following equation;

$$\frac{C_e}{q_e} = \frac{1}{K_L q_m} + \frac{1}{q_m} C_e \qquad (6)$$

Where C_e is the equilibrium concentration in the solution (mg/L), q_e the amount of metal ion adsorbed on adsorbent NCS (mg/g), q_m is amount of metal ion for a formation of a monolayer adsorbate on adsorbent surface (mg/g), K_L is Langmuir equilibrium constant that depends on the absorbed energy (mg /L). The essential characteristics of the Langmuir isotherm can be expressed by a dimensionless constant called the separation factor R_L that calculated as follow;

Where, C_o is initial concentration of adsorbate (mg/g), R_L values indicate the adsorption to be unfavorable when $R_L > 1$, linear when $R_L = 1$, favorable when $0 < R_L < 1$ and irreversible when $R_L = 0$.

The Freundlich isotherm is another popular isotherm that is used widely to express adsorption equilibrium at constant temperature [7].

The linearized Freundlich adsorption model is shown by the following equation:

$$\log qe = \log k_F + \frac{1}{n}(\log C_e) \qquad (8)$$

Where, K_F is Freundlich isotherm constant that shows adsorption potential and n is Freundlich equilibrium constant that expresses the binding energy between the adsorbent and metal ions. The isotherm constants for these models were found by a linear regression and the results are shown in Table2 and Fig.5(a-b)The data values indicate that the adsorption data for Fe (II) and Mn (II) removal fitted well within the Langmuir and the Freundlich isothermal curve for the concentration studied. However, the higher correlation coefficient obtained from Freundlich model (R^2 = 0.985, 0.979) for Fe (II) and Mn (II) respectively compared to Langmuir curve (R^2 = 0.93,0.95) for Fe (II)and Mn(II), respectively, suggests that the adsorption was taken place on the heterogeneous surface of the adsorbent much better than the monolayer adsorption. The value of R_L calculated for Fe (II) and Mn (II) concentrations was 0.115 and 0.217, respectively, that means the adsorption of both of metal ions on NCS is a favorable process. For the Freundlich constant, n for Fe (II) and Mn (II) were 2.58 and 1.69 g/l, respectively, these values of n represent an appropriate adsorption.

Table 2. Langmuir and the Freundlich equations parameters for removal Fe(II)and Mn(II)

	parameter	Fe(II)	Mn(II)
Langmuir Isotherm Results	q_m (mg/g)	133.33	99.3
	k_L (l/mg)	0.064356	0.33665
	R^2	0.93	0.95
	R_L	0.115	0.217
Freundlich Isotherm Results	n	2.58	1.69
	k_F	3.807	2.442
	R^2	0.979	0.985

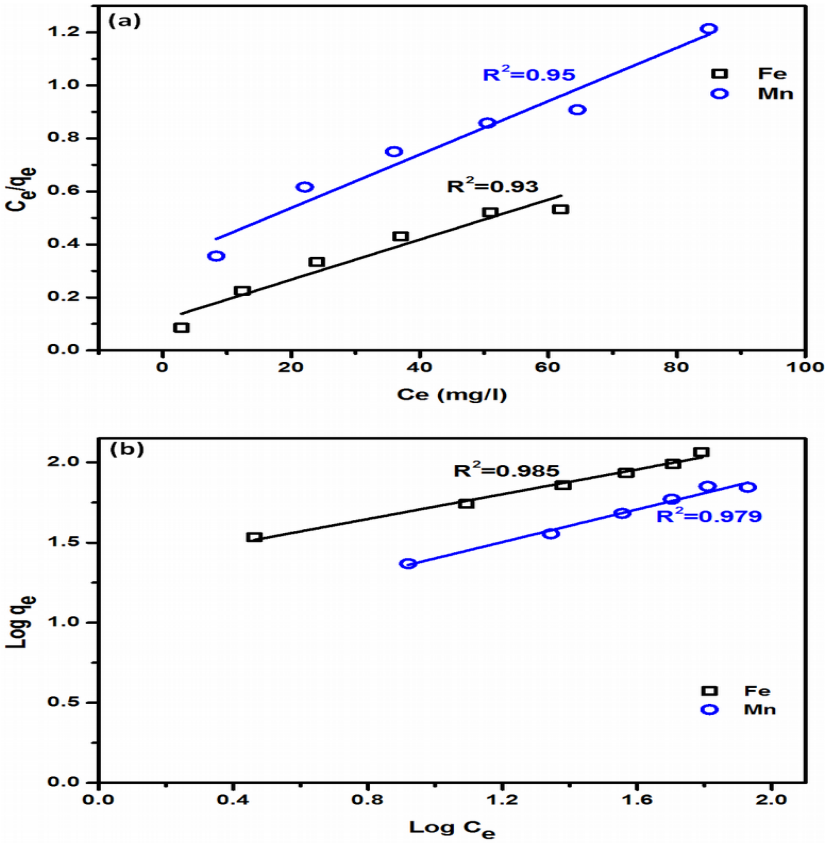

Fig.5. Langmuir (a) and Freundlich (b) isotherm models for the adsorption of Fe and Mn on nanochitosan.

5.4. Adsorption Kinetics

A suitable adsorbent for water treatment must not only have a high capacity but also a fast adsorption rate. Adsorption rate is one of the important properties of adsorbent. Kinetic models are used to survey the controlling parameters of adsorption processes, such as adsorption rate, chemical reaction, and diffusion mechanisms. Fig.6 (a-b) shows the effect of contact time on of Fe(II)and Mn (II) adsorption by NCS. For kinetics study, the models of pseudo-first order and pseudo-second order were used. The pseudo-first order model equation is;

$$\text{Log}(q_e - q_t) = \log q_e - k_1 t \qquad (9)$$

Where q_t (mg/g) is amounts of metal ion adsorbed at time "t", q_e is amounts of metal ion adsorbed at equilibrium, and K_1 is the constant coefficient of pseudo-first-order rate of adsorption (min^{-1}).by the value, k_1 is obtained by plotting $\log(q_e - q_t)$ against t. The linear form of pseudo-second-order model is given by the following equation;

$$\frac{t}{q_t} = \frac{1}{k_2 q_e^2} + \frac{1}{q_e} t \qquad (10)$$

Where K_2 is the rate constant of pseudo-second order adsorption, k_2 is also obtained by plotting t/q_t against t. The fitted parameters of the two kinetic models are reported in Table (3). The experimental q_e values for both metal ions were closer to the calculated q_e values obtained from the second order kinetic plots compared to those of the first order kinetic plots and The values the correlation coefficient R^2 for both metal ions from the linear plots show slightly different (Table 3). These indicated the adsorption kinetics followed the pseudo-second-order kinetics.

Table 3. Kinetic pseudo-first –second order equations parameters for removal Fe(II)and Mn(II)

Isotherm	parameter	Fe(II)	Mn(II)
Pseudo-first-order	K_1 (min^{-1})	0.00523	0.00362
	q_e (mg/g)	2.8	1.82
	R^2	0.959	0.936
Pseudo-second-order	K_2 (g/mg.·min)	5.836×10^{-5}	5.778×10^{-5}
	R^2	0.989	0.899
	q_e calc. (mg/g)	185.873	148.588
	q_e exp. (mg/g)	116.2	70

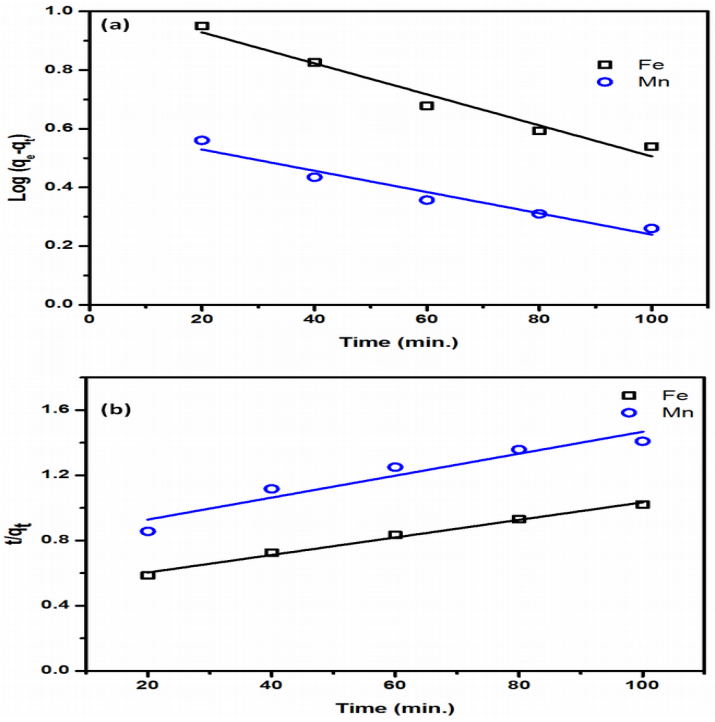

Fig.6: (a) Pseudo-first-order kinetic model –(b) Pseudo-second-order kinetic models for the adsorption

6. CONCLUSION

Chitosan is extracted from the locally available shrimp shell waste using inexpensive chemicals with DDA75% and M.wt 3923 characterized using FTIR and XRD and converted to the nano size by ionic gelation method using TPP to increase its surface area to enhance adsorption capacity characterized using particle size analyzer, TEM and SEM images showed that NCS it was succefuly prepared .batch experiments with different factors include pH, adsorbent dose ,initial concentration and contact time used for removal Fe (II)and Mn(II) and adsorption isotherms Langmuir and Freundlich was used to study the distribution of metal ions on the surface of nano chitosan and pseudo first-second order as adsorption kinetics used to know the adsorption rate, the sorption capacity of chitosan nanoparticles is high and the adsorbent favors multilayer adsorption. The kinetics studies show that the adsorption follows the pseudo-second-order kinetics. The choice of chitosan nanoparticles for removal Fe (II)and Mn(II) metal ions is considered an economic inexpensive substance used as chemical adsorbent for water treatment

REFERENCES

1. Reiad, N.A., et al., *Adsorptive removal of iron and manganese ions from aqueous solutions with microporous chitosan/polyethylene glycol blend membrane.* Journal of Environmental Sciences, 2012. **24**(8): p. 1425-1432.
2. Crossgrove, J. and W. Zheng, *Manganese toxicity upon overexposure.* NMR Biomed, 2004. **17**(8): p. 544-553.
3. Vries, D., et al., *Iron and manganese removal: Recent advances in modelling treatment efficiency by rapid sand filtration.* Water Res, 2017. **109**: p. 35-45.
4. Gerente, C., et al., *Application of Chitosan for the Removal of Metals From Wastewaters by Adsorption—Mechanisms and Models Review.* Critical Reviews in Environmental Science and Technology, 2007. **37**(1): p. 41-127.
5. Guibal, E., et al., *A Review of the Use of Chitosan for the Removal of Particulate and Dissolved Contaminants.* Separation Science and Technology, 2006. **41**(11): p. 2487-2514.
6. Liu, C., et al., *Efficient removal of Cd(ii) ions from aqueous solutions via visible capturing.* RSC Adv., 2016. **6**(44): p. 38430-38436.
7. Seyedi, S.M., et al., *Comparative Cadmium Adsorption from Water by Nanochitosan and Chitosan.* International Journal of Engineering and Innovative Technology (IJEIT), 2013.
8. Gamage, A. and F. Shahidi, *Use of chitosan for the removal of metal ion contaminants and proteins from water.* Food Chemistry, 2007. **104**(3): p. 989-996.
9. Honarkar , H. and M. Barikani *Applications of biopolymers I: chitosan.* Monatshefte für Chemie - Chemical Monthly, 2009. **140**(12): p. 1403-1420.
10. Ahing, F.A. and N. Wid, *Optimization of shrimp shell waste deacetylation for chitosan production.* International Journal of advanced and applied sciences, 2016. **3**(10): p. 31-36.
11. Cacciari, M., M.L. Mangano, and P. Nason, *Gluon PDF constraints from the ratio of forward heavy-quark production at the LHC at [Formula: see text] and 13 TeV.* Eur Phys J C Part Fields, 2015. **75**: p. 70-73.
12. Bhumkar, D.R. and V.B. Pokharkar, *Studies on Effect of pH on Cross-linking of Chitosan With Sodium Tripolyphosphate: A Technical Note.* AAPS PharmSciTech, 2006. **7**: p. E1-E6.
13. Kunjachan, S. and S. Jose, *Understanding the mechanism of ionic gelation for synthesis of chitosan nanoparticles using qualitative techniques.* Asian Journal of Pharmaceutics, 2010. **4**(2): p. 148-153.
14. Agarwal, M., D. Nagar, and N. Srivastava, *Chitosan Nanoparticles based Drug Delivery.* International Journal of Advanced Multidisciplinary Research, 2015. **2**: p. 1-13.
15. Fan, W., et al., *Formation mechanism of monodisperse, low molecular weight chitosan nanoparticles by ionic gelation technique.* Colloids Surf B Biointerfaces, 2012. **90**: p. 21-27.
16. Ali, S.W., M. Joshi, and S. Rajendran, *Synthesis and Characterization of Chitosan Nanoparticles with Enhanced Antimicrobial Activity.* International Journal of Nanoscience, 2011. **10**(04n05): p. 979-984.
17. Younes, I. and M. Rinaudo, *Chitin and chitosan preparation from marine sources. Structure, properties and applications.* Mar Drugs, 2015. **13**(3): p. 1133-1174.
18. Benhabiles, M.S., et al., *Antibacterial activity of chitin, chitosan and its oligomers prepared from shrimp shell waste.* Food Hydrocolloids, 2012. **29**(1): p. 48-56.
19. Yuan, Y., et al., *Deacetylation of Chitosan: Material Characterization and in vitro Evaluation via Albumin Adsorption and Pre-Osteoblastic Cell Cultures.* Materials, 2011. **4**(12): p. 1399-1416.

20. Vaezifar, S., et al., *Effects of Some Parameters on Particle Size Distribution of Chitosan Nanoparticles Prepared by Ionic Gelation Method.* Journal of Cluster Science, 2013. **24**(3): p. 891-903.
21. Qi, L. and Z. Xu, *Lead sorption from aqueous solutions on chitosan nanoparticles.* Colloids and Surfaces A: Physicochemical and Engineering Aspects, 2004. **251**(1-3): p. 183-190.
22. Puvvada1, Y.S., *Extraction of chitin from chitosan from exoskeleton of shrimp for application in the pharmaceutical industry.* International Current Pharmaceutical Journal, 2012.
23. Hossain, M.S., *Production and characterization of chitosan from shrimp waste.* J. Bangladesh Agril. Univ, 2014.
24. Alishahi, A., et al., *Enhancement and Characterization of Chitosan Extraction from the Wastes of Shrimp Packaging Plants.* Journal of Polymers and the Environment, 2011. **19**(3): p. 776-783.
25. Alsharabasy, A.M., *Semi-synthesis of Chitosan with High Molecular Weight and Enhanced Deacetylation Degree.* Polymer science, 2016. **02**(02).
26. K, B. and R. Ara Begum E, *Chitosan A Low Cost Adsorbent for Electroplating Waste Water Treatment.* Journal of Bioremediation & Biodegradation, 2016. **07**(03).
27. Radnia, H., et al., *Adsorption of Fe(II) ions from aqueous phase by chitosan adsorbent: equilibrium, kinetic, and thermodynamic studies.* Desalination and Water Treatment, 2012. **50**(1-3): p. 348-359.
28. Zareie, C., *Preparation of Nanochitosan as an Effective Sorbent for the Removal of Copper Ions from Aqueous Solutions.* International Journal of Engineering, 2013. **26**(8 (B)).
29. Chattopadhyay, D.P. and M.S. Inamdar, *Studies on Synthesis, Characterization and Viscosity Behaviour of Nano Chitosan.* Research Journal of Engineering Sciences, 2012. **1**(4): p. 9-15.
30. Ahing , F.A. and N. Wid *Extraction and Characterization of Chitosan from Shrimp Shell Waste in Sabah.* Transactions on Science and Technology 2016. **3**: p. 227 - 237.
31. O-T, W., *The infrared spectra of complex molecules. Vol. 1, 3rd. edn., LJ Bellamy, Chapman and Hall, London, 1975, pp. xix+ 433, price£ 8.00.* Journal of Molecular Structure, 1976. **34**: p. 315-315.
32. Sivakami, M.S., et al., *Preparation and characterization of nano chitosan for treatment wastewaters.* Int J Biol Macromol, 2013. **57**: p. 204-212.
33. Huang, K.-S., Y.-R. Sheu, and I.-C. Chao, *Preparation and Properties of Nanochitosan.* Polymer-Plastics Technology and Engineering, 2009. **48**(12): p. 1239-1243.
34. Liu, H. and C. Gao, *Preparation and properties of ionically cross-linked chitosan nanoparticles.* Polymers for Advanced Technologies, 2009. **20**(7): p. 613-619.
35. Koukaras, E.N., et al., *Insight on the formation of chitosan nanoparticles through ionotropic gelation with tripolyphosphate.* Mol Pharm, 2012. **9**(10): p. 2856-2862.
36. Vila, A., et al., *Low molecular weight chitosan nanoparticles as new carriers for nasal vaccine delivery in mice.* European Journal of Pharmaceutics and Biopharmaceutics, 2004. **57**(1): p. 123-131.
37. Shekhawat, A., et al., *Removal of Cd(II) and Hg(II) from effluents by ionic solid impregnated chitosan.* Int J Biol Macromol, 2017.
38. Hall and Christine, *Evaluation of Iron and Manganese Control for a Volcanic Surface Water Supply Treated with Conventional Coagulation, Sedimentation and Filtration Processes.* Electronic Theses and Dissertations, 2014.
39. Crini, G. and P.-M. Badot, *Application of chitosan, a natural aminopolysaccharide, for dye removal from aqueous solutions by adsorption processes using batch studies: A review of recent literature.* Progress in Polymer Science, 2008. **33**(4): p. 399-447.